Carpathian Journal of Earth and Environmental Sciences, July 2017, Vol. 12, No. 2, p. 329 - 334

FLOOD HAZARD MONITORING USING GIS AND REMOTE SENSING OBSERVATIONS

Maxim ARSENI*, Adrian ROŞU, Corina BOCĂNEALĂ, Daniel-Eduard CONSTANTIN & Lucian Puiu GEORGESCU

*Faculty of Science and Environment, European Center of Excellence for the Environment, "Dunarea de Jos" University of Galati, 111, Domneasca Street, RO-800201, Galati, Romania, *Corresponding author: maxim.arseni@ugal.ro, rosu_adrian_90@yahoo.ro, Corina.Bocaneala@ugal.ro, condaned@yahoo.com, daniel.constantin@ugal.ro, lucian.georgescu@ugal.ro*

Abstract: Flood is considered to be a major natural disaster which affects many parts of the world. Geographical Information System (GIS) can be used to visualize the extent of flood and also to analyze the risk of disasters. The objective of this study is to generate a flood hazard map using satellite image data from Landsat 5. To characterize the land cover types it was used an innovative Semi-automated Classification Processing (SCP) tool. An experimental study was conducted on the downstream of Prut River Romania, more exactly nearby Cârja (Romania) village situated on the right bank and Goteşti (Moldova) village situated on the left bank of Prut river. To monitor the effects of flood was used the supervised classification of two Landsat 5 images acquired on 2010 when a severe flood was affected the above mentioned area. This research presents a very rapid and affordable method of flood monitoring that could be very useful for the emergency management plan of the local authorities.

Keywords: land cover, flood monitoring, Landsat 5, automated processing, hazard map

1. INTRODUCTION

Land cover describes the physical cover of the Earth's surface including vegetation and non-vegetation parts. The detailed knowledge of land cover can give a solution for sustainable planning in the context of agriculture, urban development and nature conservation (Huth et al., 2012). Land cover information from the satellite imagery is a widely-used tool for large area environmental monitoring and analyses of change processes on the Earth's surface (Cihlar, 2000) and this are complementary to local and regional airborne observation (Tralli et al., 2005). Global networks for the assessment of the impact of climate changes (GTOS – Global Terrestrial Observing System, GCOS – Global Climate Observing System etc.) consider that the land cover is one of 13 essential climate variables beside biomass, leaf area index, fire disturbance, water use etc. (Schaaf et al., 2008).

Flood is considered to be the most common natural disaster worldwide during the past decades, producing many environmental and socio-economic consequences within the affected flood plain. The impacts of severe floods are huge losses in human life's, as well as economic dimensions. In Europe, in the 20th century, floods directly caused 9500 fatalities and losses assessed at 70 billion euro (Dysarz et al., 2015). Flood hazard maps are useful for planning the future direction of city growth, and are usually used to identify flood-susceptible areas. Flood is a function of the location, intensity, volume, and duration of precipitation (Zhou et al., 2000). Flood hazard mapping by LANDSAT data is known as an economical and efficient method for mapping flood hazard and deals with the problem of inadequate data source in developing countries. Geographic information system (GIS) and remote sensing techniques contributed significantly to the natural hazards analysis.

2. STUDY AREA

Prut hydrographic space is situated in North-Eastern part of Romania and West part of the Republic of Moldova (Fig. 1) (Radu, 2009).

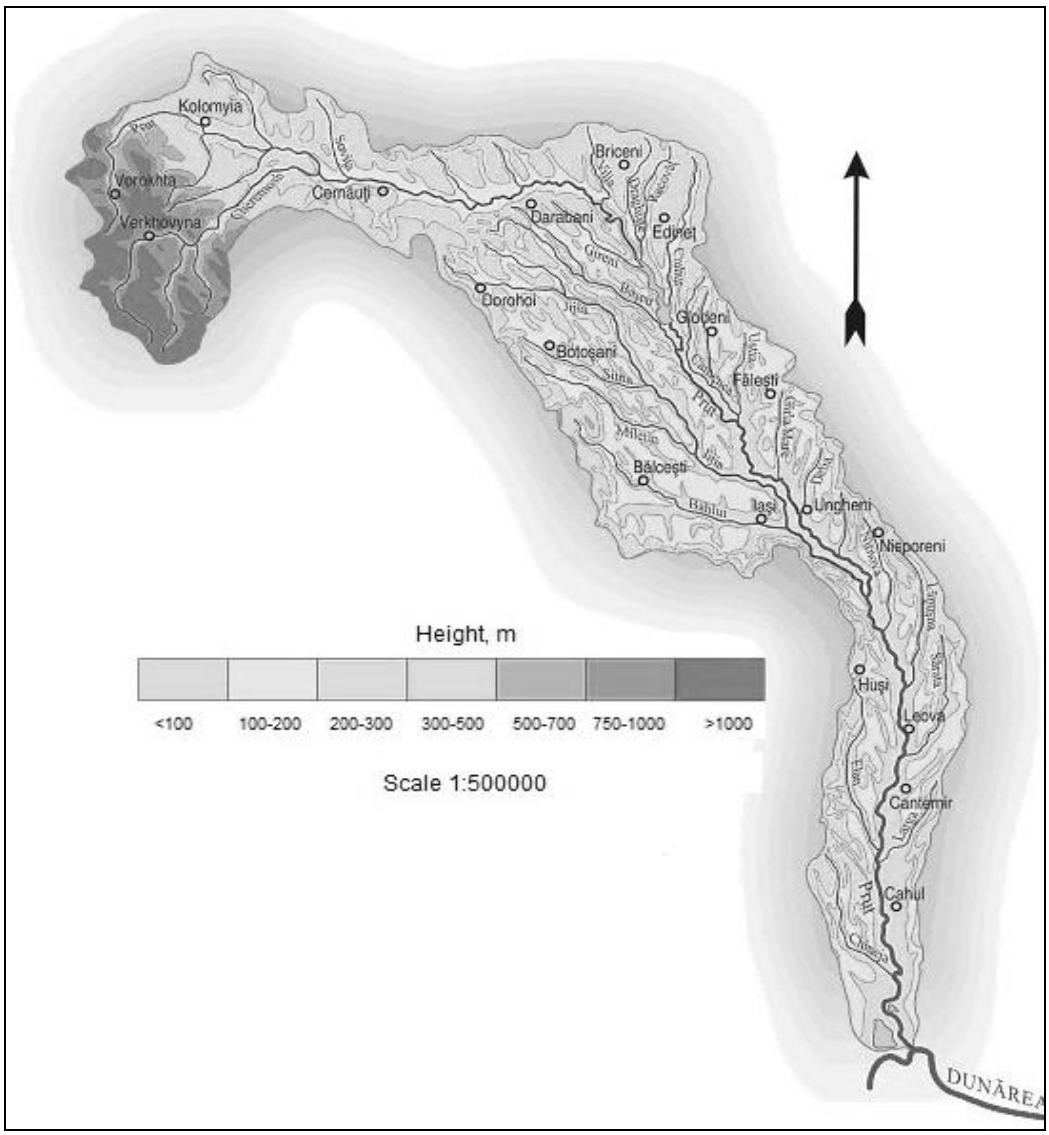

Figure 1. The map of the Prut River basin (from https://www.icpdr.org/main/activities-projects/flood-action-plans)

It is neighboring at west and south Siret basin, comprises integrally: Botosani (90%), Iasi (83%) and Vaslui (100%) counties and partially: Neamt, Bacau, Vrancea and Galati.

The multiannual average discharges of Prut growth from 78.1 m^3/s in Radauti section, at 86.7 m^3/s in Ungheni section and 105 m^3/s (3314 $mn.m^3$) at the confluence with Danube. The main tributary of Prut, Jijia, brings in 10 m^3/s (316 $mn.m^3$). For Barlad, the average discharge varies from 9.48 m^3/s (300 $mn.m^3$) in Bârlad section to 11 m^3/s (347 $mn.m^3$) at the confluence with Siret. In table 1 are represented 4 significant events which have caused major flood along the Prut River.

These floods were very significant considering the criteria of the produced damages:

1. Human health consequences (casualties);
2. Consequences on economic activity;
3. Consequences on the environment;
4. Consequences on cultural heritage.

The study area chosen for this research is located in downstream of Prut River. The total length of the study area is about 50 km. The surface elevation of the area range between 60 and 100 m. The study area is considered to have a Mediterranean climate with an annual average of precipitation of 892.5mm. The daily minimum average of temperature is 5^0C during the winter, and daily maximum temperature is 22^0C during the summer.

Table 1. Historical events identified on Prut River (from www.rowater.ro)

Management authority	**Event name**	**Date of the flood**
Water Basin Administration Prut-Barlad	Prut June 1985	17.06.1985
	Tecucel Sept. 2007	05.09.2007
	Prut July 2008	24.07.2008
	Prut June 2010	21.06.2010

3. METHODOLOGY

The studied area was affected by a major flood by June 21st, 2010 (Fig. 2).

For flood monitoring we classified a Landsat image acquired on 01.05.2010 (before the flood) and a Landsat image acquired on 14.08.2010 (during the flood), in order to assess the land cover change using a semi-automatic approach. The following workflow (Fig. 3) illustrates the main phases of semi-automatic classification used for this research.

The main purpose of the study is to define water defining a classification threshold in order to identify only those pixels that are very similar to collected spectral signatures.

First of all it was made the conversion of raster bands to the surface reflectance, performing the image-based atmospheric correction using the DOS (Dark Object Subtraction) method, which aims to improve the classification results.

Figure 2. Significant flood on July 21, 2010

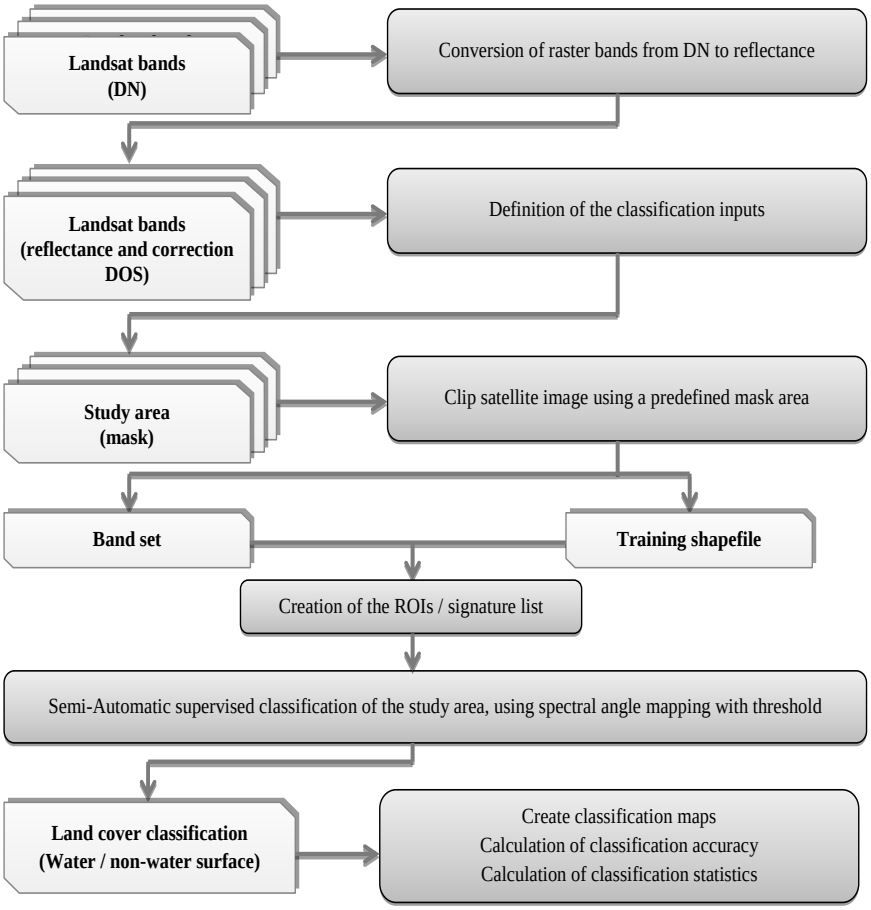

Figure 3. Workflow of the main phases of classification

The spectral reflectance properties were analyzed in order to identify the pixels that characterize the water surface. Remote sensing technique is based on the measurement of reflected or emitted radiation from different bodies (Demirkesen et al., 2007). Objects having different surface features reflect or absorb the sun's radiation in different ways. The reflectance properties of an object depend on the particular materials and its physical and chemical state, the surface roughness as well as the geometric circumstances. These differences make it possible to identify different earth surface attributes or materials by analyzing their spectral reflectance (Lunetta et al., 2006) pattern or spectral signatures (Fig. 4).

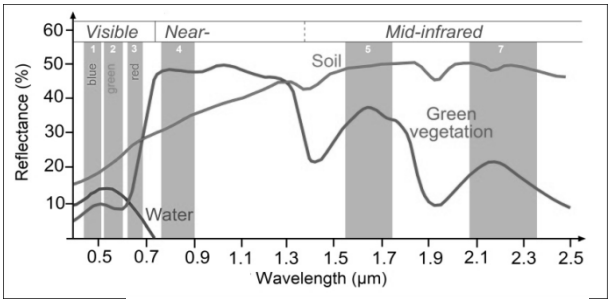

Figure 4. Reflectance of water, soil and vegetation in different wavelengths and Landsat TM channels

As the figure 4 shows, the water curve is characterized by a high absorption at near infrared wavelengths range and beyond. Because of this absorption property, water bodies as well as features containing water can easily be detected, located and delineated with remote sensing data.

For a better distinction it was used the 4-3-2 color composite scheme: the band 4 for the red band, the band 3 for the green band, and band 2 for the blue band (Fig. 5 a, b).

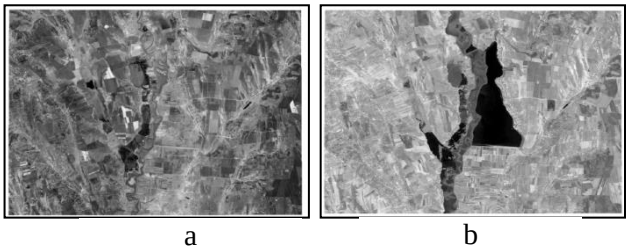

a b

Figure 5. Color composite scheme 4-3-2: a – before flood, b – after flood

After the conversion of raster band to surface reflectance it was collected the ROIs (region of interest) that define the land cover class of water. To improve the results, it is important to collect ROIs of dark water and light water.

In order to distinguish only the water, the image was processed using Spectral Angle Mapping algorithm with a threshold. Depending on the threshold value, pixels are classified as water if the angle between the spectral signatures thereof and the spectral signatures collected in the previous step are below the threshold value. If the maximum threshold value is not defined correctly the non-water pixels are going to be incorrectly classified as water.

4. RESULTS

For the flooded area analysis, were collected spectral signature from the first Landsat image, and applied to the second image. In order to determine the water and non-water surface were used two classes (Fig. 6 a, b). The black color represents the non-water surfaces (class 0), and the white color – the water surfaces (class 1). Statistical results are presented in table 2.

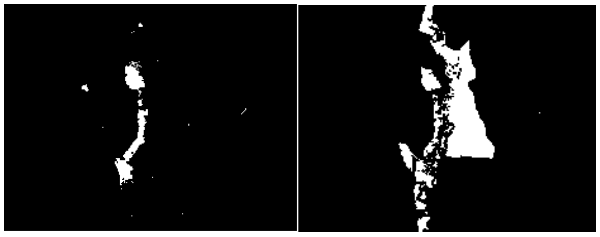

a b

Figure 6. Classification of water and non-water surfaces: a – before flood, b – after flood

Table 2. Classification report before and after flood

Before flood			
Class	Pixel sum	Percentage [%]	Area [m^2]
0.0	660126	97.6	59413400
1.0	16674	2.4	15006600
Total	676800	100	609120000
After flood			
Class	Pixel sum	Percentage [%]	Area [m^2]
0.0	613124	90.6	551811600
1.0	63676	9.4	57308400
Total	676800	100	609120000

For the assessment of flooded was calculated the land cover change between this two classifications.

$$A_{nwb}=A_t-A_{wb}\ [km^2]\ (1)$$

$$A_{nwa}=A_t-A_{wa}\ [km^2]\ (2)$$

$$A_f=A_{wa}-A_{wb}=A_{nwa}-A_{nwb}\ [km^2]\ (3)$$

From above formula results that the flooded area covers about 4230 sq. km.

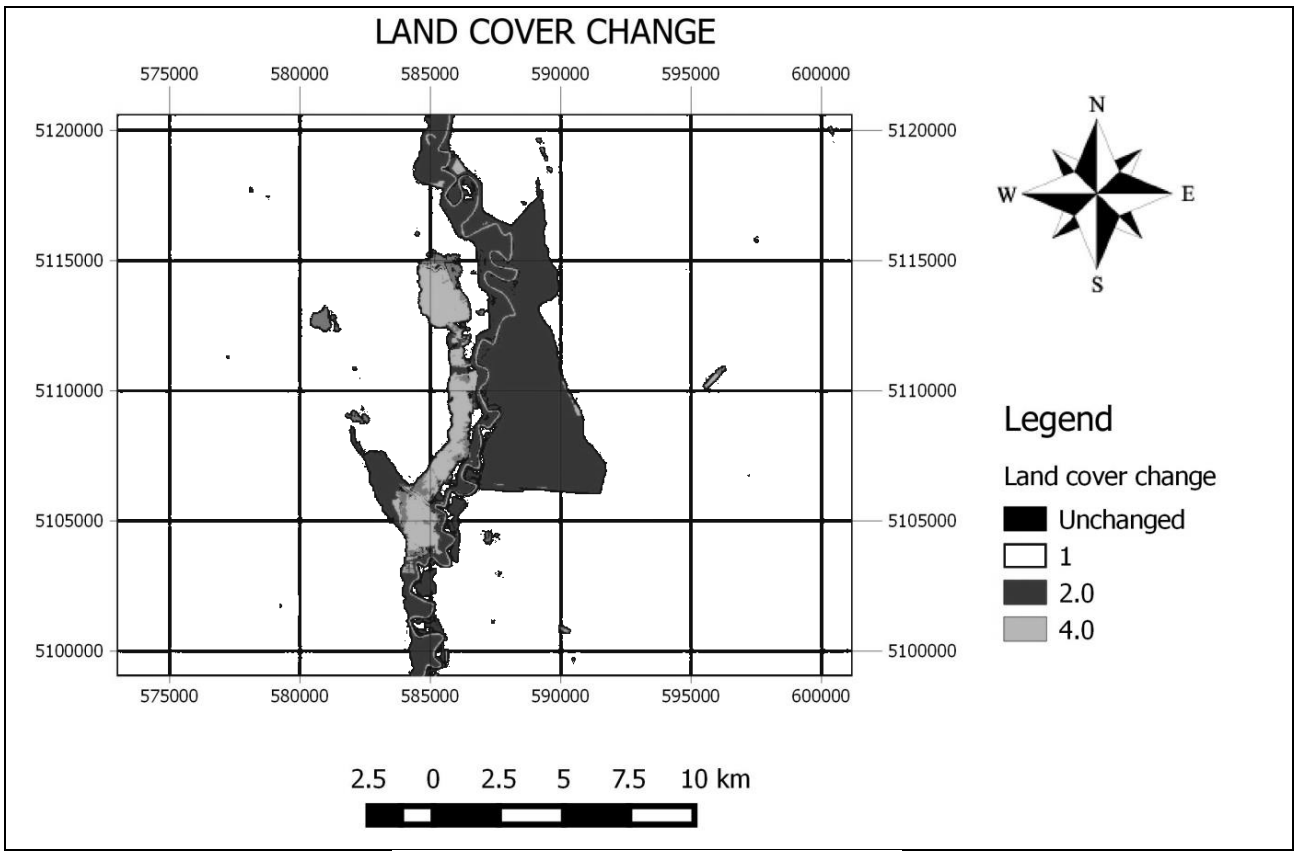

Figure 7. The flood extent map on 21 July 2010

Using the TM data and the above described method, it was created a map representing flooded areas in Cârja (Romania) village and Goteşti (R. Moldova) village (Fig. 7).

5. CONCLUSION

Remote sensing technologies are very useful in flood monitoring damages evaluation. Remotely sensed data play an integral role in reconstructing the recent history of the land surface and in predicting hazards due to flood and landslide events. Also, if we use satellite remote sensing data we can increase are complemente the ground-based network data, and in situ and field observations for disaster assessment and response.

A simple and efficient method for mapping flood extent has been presented. With limited ground observation, most flooded and non-flooded areas derived from the analysis were verified. This method was based on a comparison of the reflectance feature of the water surface versus non-water surface on a pair of Landsat 5 image (one acquired before and other during the flood event).

The total flooded area derived from the satellite images, on 26 July 2010 for Cârja (Romania) village and Goteşti (R.Moldova) village were 4230 km^2 or approximately 7% of the total studied area. The SCP tool is an efficient device for the semi-automatic classification of remote sensing images, which provides several tools for the images processing, the post processing of classifications, and the raster calculation.

However, it should be noted that the successful application of Landsat images for flood damage assessment demonstrated the ability and the potential of remote sensing technique in monitoring floods and for estimating the flood regimes. Satellite-derived flood inundation maps produced in near-real time are invaluable to state or national agencies for disaster monitoring and relief efforts. More research is required to integrate other data such as digital topographic data and river networks measurements in order to improve the spatial accuracy and develop new algorithms for flood analyzing.

REFERENCES

Cihlar, J. 2000. *Land cover mapping of large areas from satellites: status and research priorities.* International journal of remote sensing, 21(6-7), 1093-1114.

Demirkesen, A. C., Evrendilek, F., Berberoglu, S., & Kilic, S. 2007. *Coastal flood risk analysis using Landsat-7 ETM+ imagery and SRTM DEM: A case study of Izmir, Turkey*. Environmental

monitoring and assessment, 131(1-3), 293-300.

Dysarz, T., Wicher-Dysarz, J., & Sojka, M., 2015. *Assessment of the Impact of New Investments on Flood Hazard-Study Case: The Bridge on the Warta River near Wronki.* Water, 7(10), 5752-5767.

Huth, J., Kuenzer, C., Wehrmann, T., Gebhardt, S., Tuan, V. Q., & Dech, S., 2012. *Land cover and land use classification with TWOPAC: Towards automated processing for pixel-and object-based image classification.* Remote Sensing, 4(9), 2530-2553.

Lunetta, R. S., Knight, J. F., Ediriwickrema, J., Lyon, J. G., & Worthy, L. D., 2006. *Land-cover change detection using multi-temporal MODIS NDVI data.* Remote sensing of environment, 105(2), 142-154.

Radu, G., 2009. *Hydrological features of the lower Prut floodplain.* Air and water. Components of the Environment. (Aerul si Apa. Componente ale Mediului), 179.

Schaaf, C. B., Barry, R. G., Brady, M., Brown, J., CEOS, Christiansen, H. H., Cihlar, J., Clow, G., Csiszar, I., Dolman, H., Famiglietti, J., Fritz, G., Gobron, N., Grabs, W., Haeberli, W., Healy, E., Martin, H., Martin, H., Hooheveen, J., Kalensky, D., Latham, J., Looser, U., Mintier, S., Monteduro, M., Nelson, F. E., Paul, F., Romanovsky, V., Sacco, G., Schmullius, C., Sessa, R., Smith, S. L., Werf, G., Woodcock, C., Wulder, M. & Zemp, M., 2008. *Terrestrial Essential Climate Variables: Climate Change Assessment, Mitigation and Adaptation.* FAO: Rome, Italy.

Tralli, D. M., Blom, R. G., Zlotnicki, V., Donnellan, A., & Evans, D. L. 2005. *Satellite remote sensing of earthquake, volcano, flood, landslide and coastal inundation hazards.* ISPRS Journal of Photogrammetry and Remote Sensing, 59 (4), 185-198.

Zhou, C., Luo, J., Yang, C., Li, B., & Wang, S. 2000. *Flood monitoring using multi-temporal AVHRR and RADARSAT imagery.* Photogrammetric engineering and remote sensing, 66(5), 633-638.

Received at: 28. 06. 2016
Revised at: 15. 10. 2016
Accepted for publication at: 17. 11. 2016
Publised online at: 04. 01. 2017